



## Tracking studies regarding the electron model 3-5.4463 MeV of a non-linear, non-scaling, proton driver FFAG 3-10 GeV

D. Kelliher, F. Lemuet, F. Méot, G. Rees

### ► To cite this version:

D. Kelliher, F. Lemuet, F. Méot, G. Rees. Tracking studies regarding the electron model 3-5.4463 MeV of a non-linear, non-scaling, proton driver FFAG 3-10 GeV. 2006, 10 p. <in2p3-00120977>

**HAL Id: in2p3-00120977**

**<http://hal.in2p3.fr/in2p3-00120977>**

Submitted on 19 Dec 2006

**HAL** is a multi-disciplinary open access archive for the deposit and dissemination of scientific research documents, whether they are published or not. The documents may come from teaching and research institutions in France or abroad, or from public or private research centers.

L'archive ouverte pluridisciplinaire **HAL**, est destinée au dépôt et à la diffusion de documents scientifiques de niveau recherche, publiés ou non, émanant des établissements d'enseignement et de recherche français ou étrangers, des laboratoires publics ou privés.

## Tracking studies regarding the electron model 3-5.4463 MeV of a non-linear, non-scaling, proton driver FFAG 3-10 GeV.

D. Kelliher\*, F. Lemuet† F. Méot‡, G. Rees\*

\* *Rutherford Appleton Laboratory*

† *CNRS IN2P3, LPSC, Grenoble*

‡ *CEA et IN2P3, LPSC, Grenoble*

### Abstract

This paper describes the setting up of ray-tracing tools and preliminary beam dynamics studies concerning the electron model 3-5.4463 MeV of a non-linear, non-scaling proton driver FFAG 3-10 GeV.

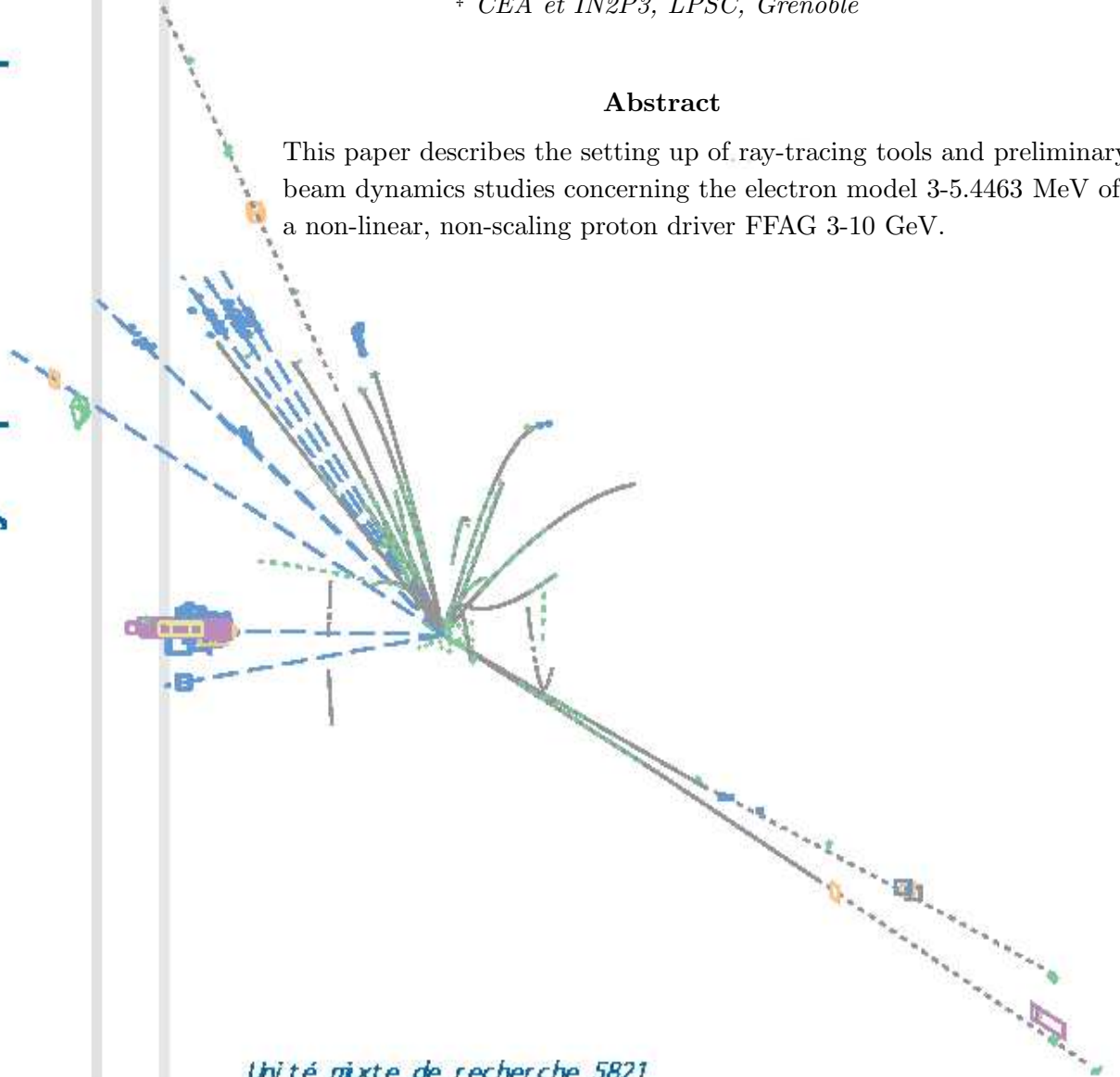


## Table des matières

1	Introduction	3
2	Fields and cell parameters	3
3	First order results	6
4	Dynamical aperture	7
5	Conclusion	8
	Appendix	10
A	Zgoubi data file	10

# 1 Introduction

The 50 Hz, 3-10 GeV, proton driver (Fig. 1) proposed for an ISS, Neutrino Factory design [1], uses a new type of FFAG, with a non-linear, non-scaling and non-isochronous, cell focusing structure [2]. An electron model 3-5.4463 MeV has been designed [3] to test various aspects of the optics. In this report we describe the setting up of the optics data files and produce preliminary beam dynamics studies concerning the effects of the non-linear magnetic fields in this electron model, using the ray-tracing code ZGOUBI [4]. Similar investigations were carried out for a non-scaling, non-linear, isochronous muon ring proposed for the 8-20 GeV fast acceleration of muons in a neutrino factory [5] and for its associated 11-20 MeV electron model [6], which can be referred to for more details on the methods.

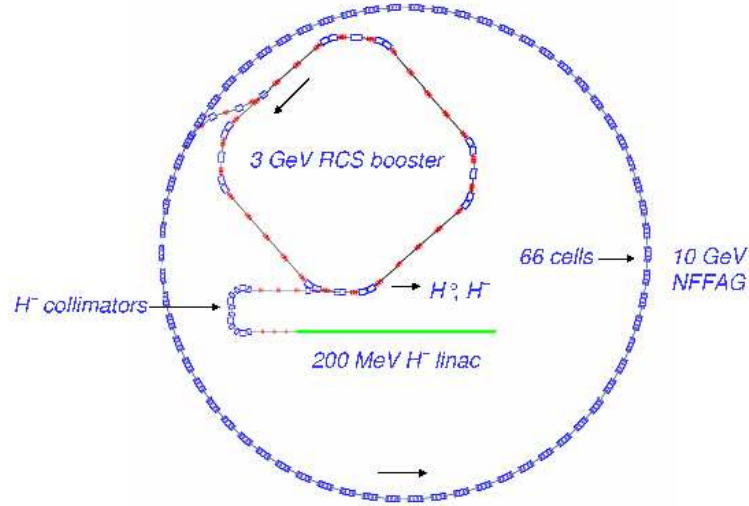


FIG. 1 – Schematic of the 3-10 GeV, NFFAG proton driver.

## 2 Fields and cell parameters

### Geometrical lattice design

The design is based on a O-bd-o-BF-o-BD-o-BF-o-BD-O cell (Fig. 2), symmetric wrt. the center of BD, built from magnets with a straight optical axis and rectangular  $B(x)$  dependence. The bd and BD magnets have parallel faces, while the second magnet, BF, has its upstream (resp. downstream) edge parrallel to the downstream (resp. upstream) edge of bd (resp. BD). Lengths are given in Fig. 2.

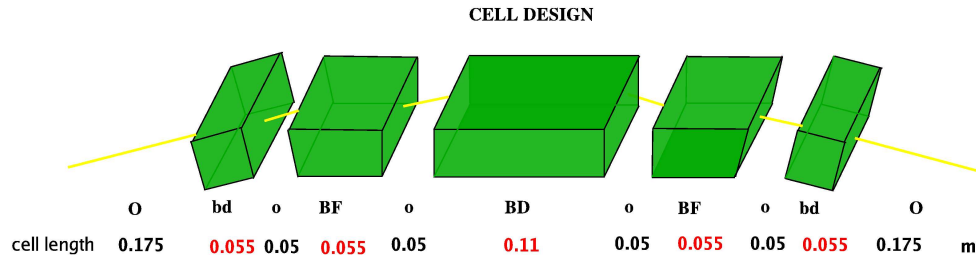


FIG. 2 – Schematic of the e-model cell. The total cell length is 0.88 m.

The rings consists of 27 cells yielding a circumference of 23.76 m (Fig. 3).

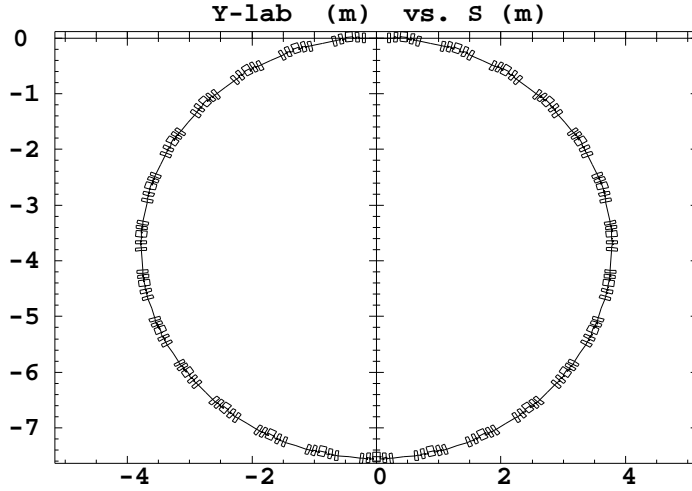


FIG. 3 – Synoptic of the FFAG non linear, non-scaling, electron model 3-5.45 MeV : 27 cells.

### Gradients and fields

The magnets are non-linear and combined function. In the case of bd and BD, they are horizontally defocusing (Fig. 8), respectively reverse and positive bend (Fig. 4). The magnet BF is horizontally focusing (Fig. 8) with positive bend (Fig. 4).

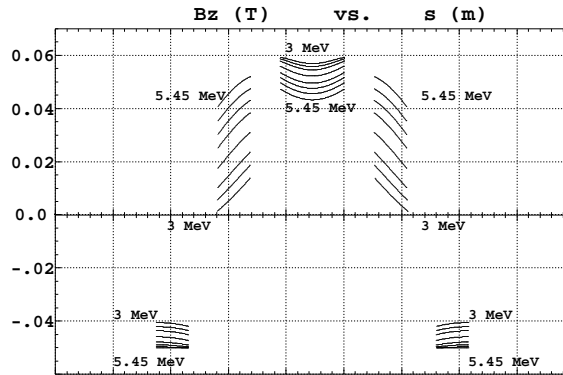


FIG. 4 – Fields seen by the particles as a function of the s coordinate in a cell.

In our simulations we use rectangular multipole with straight axis for all 3 types of magnets, including BF, and a hard-edge model. First order effect of fringe field extent on vertical motion is accounted for via a correction vertical kick of the form  $-\tan(\alpha)/\rho + FR/(6*\rho^2*\cos(\alpha))$  with  $\rho$  being the local curvature radius and  $\alpha$  the angle between the trajectory of the particle and the normal to the magnet face.

The local magnet strengths, given by the design data [3], yield the local gradients using the relation,

$$g[T/m] = \frac{p[GeV/c]K[m^{-2}]}{0.2998}$$

these gradients are approximated using three 4th degree polynomials,

$$g(x) = g_0 + g_1 x + g_2 x^2 + g_3 x^3 + g_4 x^4$$

which are next integrated so to obtain the magnetic field law in each magnet

$$b(x) = b_0 + b_1 x + b_2 x^2 + b_3 x^3 + b_4 x^4 + b_5 x^5 \quad (1)$$

Figure 5 shows the fits to the gradient data and the resulting field law compared to the design data.

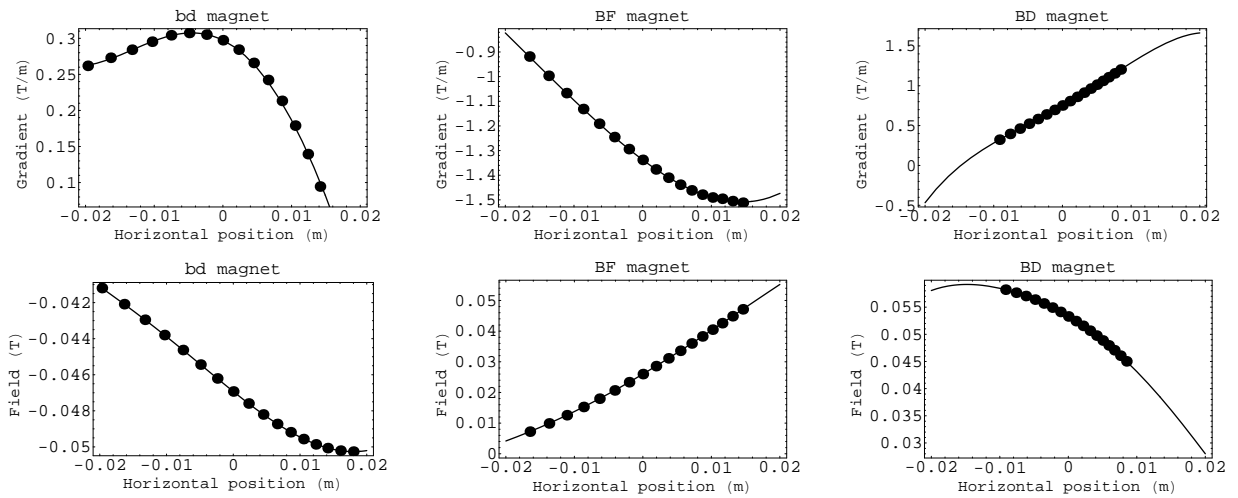


FIG. 5 – Comparison of the transverse profile of the gradients (upper figures) and the field (lower figures) in the three types of magnets, bd, BF, BD; solid lines represent the polynomial approximation of the gradients and the dots represent the design data.

The simulation of the rectangular dependence  $B(x)$  in bd, BF, BD magnets uses a classical multipole modelling of the form

$$\vec{B} = \text{grad}V_n \quad \text{with} \quad V_n(s, x, z) = (n!)^2 \left( \sum_{q=0}^{\infty} \frac{(-)^q G^{(2q)}(s)(x^2 + z^2)^q}{4^q q!(n+q)!} \right) \left( \sum_{m=0}^n \frac{\sin(m\frac{\pi}{2}) x^{n-m} z^m}{m!(n-m)!} \right) \quad (2)$$

with coefficient values  $G^{(2q)}(\text{center})$  derived from equation 1. The  $s$ -dependence  $G(s)$  allows the simulation of field fall-offs at magnet ends to be included when desired, using an Enge's fall-off model [4].

### Matching procedure

The matching procedure allows preliminary adjustment of the geometrical parameters. The constraints imposed are that the closed orbit angles in the drifts between the magnets be as close as possible to the design ones. The parameters to be varied are the closed orbit coordinates at the start of the cell, and the positioning of the magnets via rotation and horizontal translation. Three energies have been considered that correspond to injection, reference and extraction, respectively 3 MeV, 4.05 MeV, 5.4463 MeV. Satisfactory c.o. angle values have been obtained for these energies following this method, with the consequence that c.o. angles at the other energies considered in the original design take a value that agrees with the design data to the level of a percent and better.

### 3 First order results

In this section, we present first order tracking results in a cell adjusted with the matching procedure presented above. The corresponding ZGOUBI data file is in appendix A.

#### Closed orbits

Figure 6 shows closed orbits in a cell for several energies from injection to extraction. Closed orbits coordinates for 17 design energies are displayed at the beginning of the appendix A.

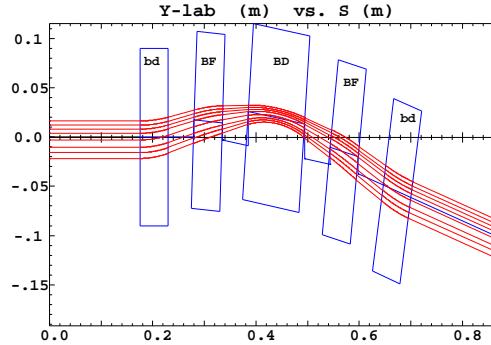


FIG. 6 – Closed orbits for the electron model 3-5.4463 MeV, as the energy increases the trajectories move from the inner to the outer part of the magnets.

#### Focusing

Figures 7, 8 show respectively periodic  $\beta$  functions at the cell end as a function of energies and  $\beta$  functions as a function of  $s$  for the reference energy 4.05 MeV.

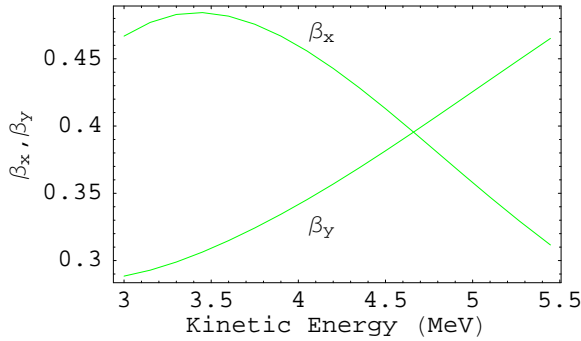


FIG. 7 – Periodic  $\beta$  values at the cell end as a function of energies.

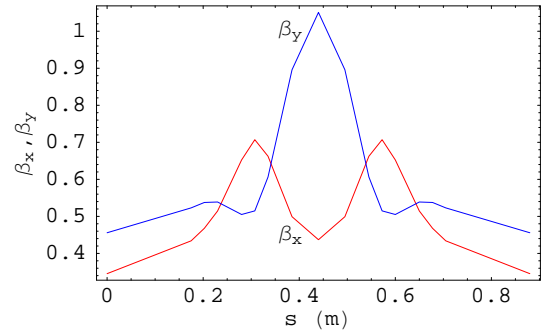


FIG. 8 –  $\beta$  functions as a function of  $s$  for the reference energy 4.05 MeV.

The design tunes per cell are constant with  $Q_x = \frac{4}{13}$  and  $Q_y = \frac{3}{13}$  (dashed lines in Fig. 9). The tunes per cell calculated with ray-tracing (green lines in Fig. 9) are slightly different with a small variation with energy. If a better agreement is needed, a matching procedure could be performed in ZGOUBI, which allows an automatic adjustment of the  $b_i$  coefficients in the multipole expansion of

equation 1 to match the tunes. Examples of this process for a muon ring and its electron model can be found in references [5], [6]. Figure 10 shows the ray-tracing total tunes expansion ( $27 \times Q_{x,y}$ ) in a fifth order tunes diagram.

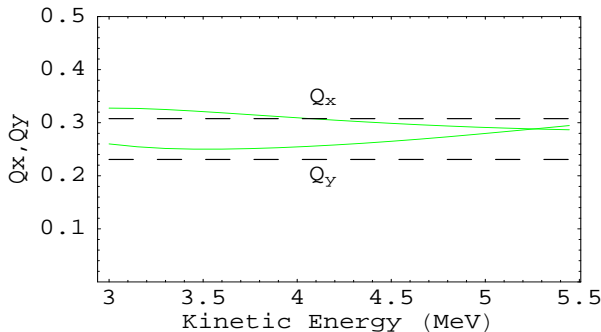


FIG. 9 – Tunes per cell as a function of kinetic energy (upper curves are horizontal tunes, lower curves vertical), green are ray-tracing results, dashed are expected values.

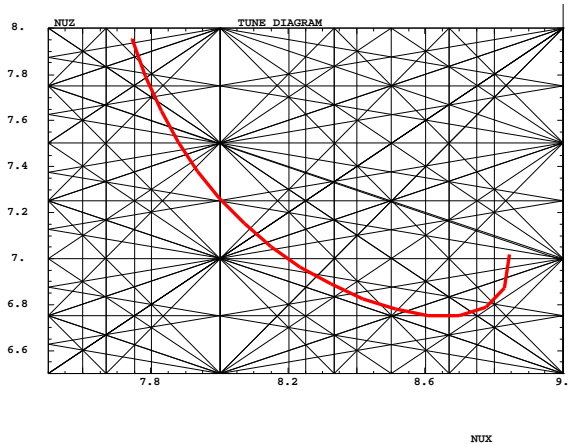


FIG. 10 – Total tunes variations in the tune diagram for  $E : 3 \rightarrow 5.4463$  MeV. Systematic resonance lines up to the fifth order are shown.

## 4 Dynamical aperture

Figure 11 shows the limit phase space trajectories obtained by multiturn tracking at injection, reference and extraction energies in case of a pure horizontal motion and when we introduce a small  $z$  motion. In that case the limits decrease sensibly, except for the injection energy for which the limit is unchanged. The total tunes corresponding to this coupled motion are displayed in the fifth order tune diagram. Figure 12 shows the vertical stability limits for the particles launched on the horizontal closed orbits.

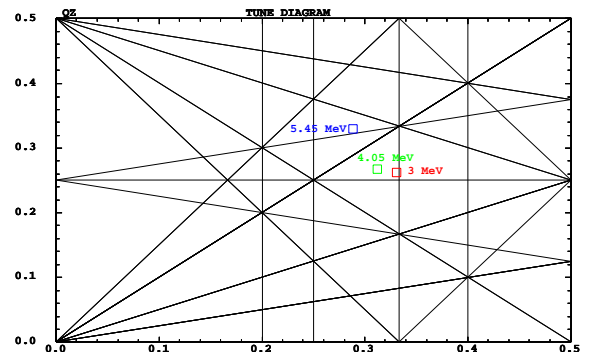
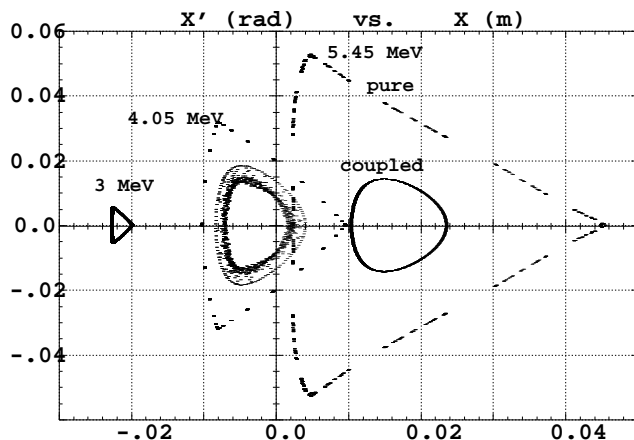


FIG. 11 – Left : 2-D motion  $(x, x')$ , 1000-cell stability limits, at 0.05 cm precision in  $x$ , at 3, 4.05, 5.45 MeV. No fringe fields. Pure (larger amplitude) and coupled (smaller amplitude) motion in the presence of a very small  $z$  component. Right : tunes per cell corresponding to coupled stability limits in the tune diagram; systematic resonances up to the fifth order.



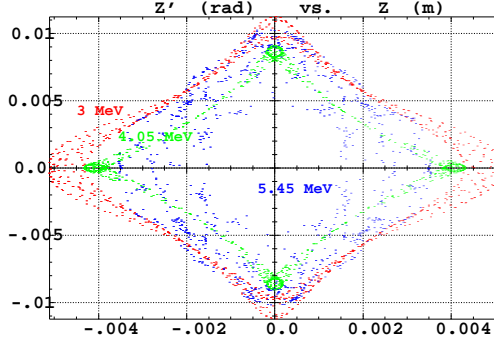


FIG. 12 – 2-D motion ( $z, z'$ ) with initial  $x$  on the closed orbits, 1000-cell stability limits, at 0.05 cm precision in  $z$ , at 3, 4.05, 5.45 MeV. No Fringe fields.

### Amplitude Detuning

Figure 13 shows the amplitude detuning in case of pure  $x$  motion. The total tunes have been calculated for the three energies starting from the closed orbits  $x_{co}$  up to the  $x_{limits}$  calculated previously (Fig. 11).

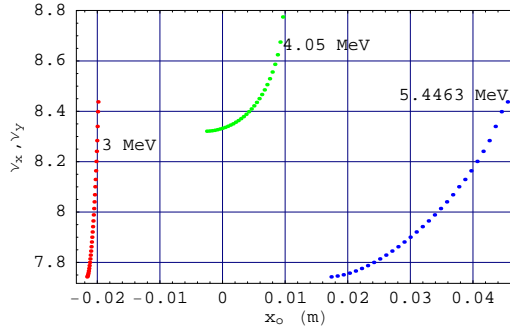


FIG. 13 – Amplitude detuning in case of pure  $x$  motion for the 3, 4.05, 5.4663 MeV energies.

### Acceptance

Figure 14 shows the horizontal and vertical dynamical apertures at 3 MeV calculated previously and their corresponding matched ellipse. The acceptances as the surfaces of these ellipses are  $\frac{\epsilon_x}{\pi} = 2.2 \cdot 10^{-6}$  m mrad and  $\frac{\epsilon_z}{\pi} = 1.8 \cdot 10^{-5}$  m mrad.

## 5 Conclusion

Preliminary tracking studies have been performed in the non-scaling, non-linear electron model of a 3-10 GeV proton driver. A more exhaustive investigation could now be carried out. Similar investigations could also be carried out on the proton driver. Further steps would include acceleration and full transmission studies as it has been performed in the isochronous muon ring and its electron model [5], [6].

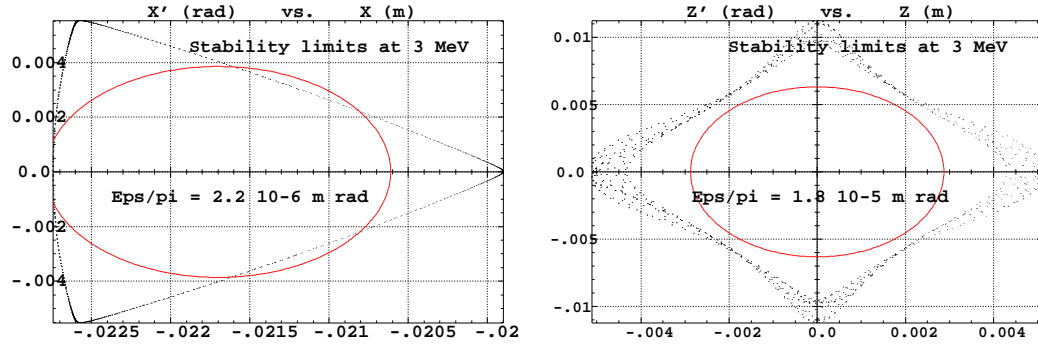


FIG. 14 – Stability limits at 3 MeV and their corresponding acceptances left for horizontal motion and right for vertical motion.

## Références

- [1] <http://www.hep.ph.ic.ac.uk/iss/>
- [2] 4 MW, 50 Hz, 3 to 10 GeV, NFFAG, Proton Driver, Grahame Rees (RAL), private communication, Dec. 2006.
- [3] 27 Cell, Electron Model for a 3 to 10 GeV, NFFAG, Proton Driver, Grahame Rees (RAL), private communication, Dec. 2006.
- [4] (a) The ray-tracing code Zgoubi, F. Meot, NIM A 427 (1999) 353-356, and also (b) Zgoubi users' guide, F. Meot and S. Valero, CEA DAPNIA SEA-97-13 and FERMILAB-TM-2010 (1997).
- [5] 6-D beam dynamics in an isochronous FFAG ring, F. Lemuet, F. Méot, G. Rees, proceedings of 2005 Particle Accelerator Conference, Knoxville, Tennessee.
- [6] 6-D beam dynamics in an electron model lattice of an isochronous FFAG, F. Lemuet, F. Méot, G. Rees, Nuclear physics B, 155 (2006) pp 330-331.

